

Synthesis and Characterization of New 19-Vertex Macropolyhedral Boron Hydrides

Joel A. Dopke, Douglas R. Powell, and Donald F. Gaines*

Department of Chemistry, University of Wisconsin—Madison, 1101 University Avenue, Madison, Wisconsin 53706

Received July 27, 1999

The new boron hydride anions $10\text{-R-B}_{19}\text{H}_{19}^-$ ($\text{R} = \text{H}, \text{Thx}$) were synthesized by the reaction of $\text{M}_2[\text{B}_{18}\text{H}_{20}]$ ($\text{M} = \text{Na}, \text{K}$) with $\text{HBRCI}\cdot\text{SMe}_2$ ($\text{R} = \text{H}, \text{Thx}$) or $\text{HBCl}_2\cdot\text{SMe}_2$ in diethyl ether. The anions are comprised of edge-sharing, *nido* 10- and 11-vertex cluster fragments, and are characterized by their ^{11}B , $^{11}\text{B}\{^1\text{H}\}$, and $^{11}\text{B}\text{--}^{11}\text{B}$ COSY NMR spectra. The salt $[(\text{Ph}_3\text{P})_2\text{N}][\text{B}_{19}\text{H}_{20}]\cdot 0.5\text{THF}$ crystallized in the triclinic space group $P\bar{1}$ ($a = 12.6344(2)\text{ \AA}$, $b = 13.5978(2)\text{ \AA}$, $c = 14.1401(2)\text{ \AA}$; $\alpha = 77.402(2)^\circ$, $\beta = 81.351(2)^\circ$, $\gamma = 73.253(2)^\circ$). Possible synthetic pathways are discussed. The dianion $\text{B}_{19}\text{H}_{19}^{2-}$ is formed by deprotonation of $\text{B}_{19}\text{H}_{20}^-$ with Proton Sponge (1,8-bis(dimethylamino)naphthalene) in THF, and is identified on the basis of its ^{11}B , $^{11}\text{B}\{^1\text{H}\}$, and $^{11}\text{B}\text{--}^{11}\text{B}$ COSY NMR spectra.

Introduction

Calculational studies by Lipscomb and co-workers have helped to fuel the pursuit of large boron hydrides by predicting that spherical *closo* clusters possessing more than 12 vertexes should be stable, although none have yet been isolated.¹ While boron hydride clusters have traditionally been thought of as deltahedral fragments of *closo* parents possessing 12 or fewer vertexes, macropolyhedral boranes have been known since the discovery of $\text{B}_{18}\text{H}_{22}$ (Figure 1) by Hawthorne et al.² Numerous examples of macropolyhedral clusters exist, with most being species in which two nominally independent cluster fragments share a single boron atom,³ one or more B–B edges,^{3–8} or a triangular B–B–B face.⁸ Only two binary boron hydride species which may be thought of as being derived from a closed parent possessing more than 12 vertexes have been reported in the literature: $\text{B}_{14}\text{H}_{20}$ ⁴ and $\text{B}_{20}\text{H}_{16}$.⁸ Recently, a number of macropolyhedral heteroborane clusters in which the heteroatom is a transition metal⁹ or a main group atom¹⁰ have appeared in the literature.

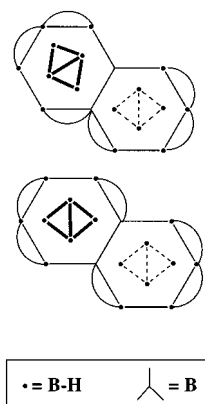


Figure 1. Stick diagrams representing the structures of *syn*- $\text{B}_{18}\text{H}_{22}$ (top) and *anti*- $\text{B}_{18}\text{H}_{22}$ (below). Arcs represent bridging hydrogens.

The most widely studied of the macropolyhedral boron hydrides is *anti*- $\text{B}_{18}\text{H}_{22}$ due largely to its stability and ready synthesis in high purity.^{11,12} The structure of *anti*- $\text{B}_{18}\text{H}_{22}$ consists of two *nido* 10-vertex clusters fused through a common edge

- (1) Bicerano, J.; Marynick, D. S.; Lipscomb, W. N. *Inorg. Chem.* **1978**, *17*, 3443. Lipscomb, W. N.; Massa, L. *Inorg. Chem.* **1994**, *33*, 5155. Lipscomb, W. N.; Massa, L. *Inorg. Chem.* **1992**, *31*, 2299.
- (2) Pitochelli, A. R.; Hawthorne, M. F. *J. Am. Chem. Soc.* **1962**, *84*, 3218.
- (3) Rathke, J.; Schaeffer, R. *J. Am. Chem. Soc.* **1973**, *95*, 3402.
- (4) Huffman, J. C.; Moody, D. C.; Schaeffer, R. *Inorg. Chem.* **1981**, *20*, 741.
- (5) Rathke, J.; Schaeffer, R. *Inorg. Chem.* **1974**, *13*, 3008. Huffman, J. C.; Moody, D. C.; Rathke, J. W.; Schaeffer, R. *J. Chem. Soc., Chem. Commun.* **1973**, 308. Rathke, J.; Moody, D. C.; Schaeffer, R. *Inorg. Chem.* **1974**, *13*, 3040. Hermanek, S.; Fetter, K.; Plešek, J. *Chem. Ind.* **1977**, 606. Friedman, L. B.; Cook, R. E.; Glick, M. D. *J. Am. Chem. Soc.* **1968**, *90*, 6862. Friedman, L. B.; Cook, R. E.; Glick, M. D. *Inorg. Chem.* **1970**, *9*, 1452. Hosmane, N. S.; Franken, A.; Zhang, G.; Rajik, R.; Smith, R. Y.; Spielsvogel, B. F. *Main Group Met. Chem.* **1998**, *21*, 6.
- (6) Simpson, P. G.; Folting, K.; Dobrott, R. D.; Lipscomb, W. N. *J. Am. Chem. Soc.* **1963**, *85*, 1879. Simpson, P. G.; Folting, K.; Dobrott, R. D.; Lipscomb, W. N. *J. Chem. Phys.* **1963**, *39*, 2339.
- (7) Simpson, P. G.; Lipscomb, W. N. *J. Chem. Phys.* **1963**, *39*, 26.
- (8) Miller, N. E.; Muettterties, E. L. *J. Am. Chem. Soc.* **1963**, *85*, 3506. Friedman, L. B.; Dobrott, R. D.; Lipscomb, W. N. *J. Am. Chem. Soc.* **1963**, *85*, 3505. Bachmann, H. R.; Nöth, H.; Rinck, R. *Chem. Phys. Lett.* **1974**, *29*, 627. Dobrott, R. D.; Friedman, L. B.; Lipscomb, W. N. *J. Chem. Phys.* **1964**, *40*, 866. Miller, N. E.; Forstner, J. A.; Muettterties, E. L. *Inorg. Chem.* **1964**, *3*, 1690. Enemark, J. H.; Friedman, L. B.; Lipscomb, W. N. *Inorg. Chem.* **1966**, *5*, 2165.
- (9) Sneath, R. L.; Little, J. L.; Burke, A. R.; Todd, L. J. *J. Chem. Soc., Chem. Commun.* **1970**, 693. Sneath, R. L.; Todd, L. J. *Inorg. Chem.* **1973**, *12*, 44. Cheek, Y. M.; Greenwood, N. N.; Kennedy, J. D.; McDondald, W. S. *J. Chem. Soc., Chem. Commun.* **1982**, 80.
- (10) Bould, J.; Kennedy, J. D.; Thornton-Pett, M. *J. Chem. Soc., Dalton Trans.* **1992**, 563. Kennedy, J. D.; Stibr, B. In *Current Topics in the Chemistry of Boron*; Kabalka, G., Ed.; Royal Society of Chemistry: Cambridge, 1994. Kennedy, J. D.; Drdákova, E.; Thornton-Pett, M. *J. Chem. Soc., Dalton Trans.* **1994**, 229. Casanova, J., Ed. *The Borane-Carborane-Carbocation Continuum*; Wiley: New York, 1998. Jelínek, T.; Cisarová, I.; Stibr, B.; Kennedy, J. D.; Thornton-Pett, M. *J. Chem. Soc., Dalton Trans.* **1998**, 2965. Jelínek, T.; Kilner, C. A.; Barrett, S. A.; Thornton-Pett, M.; Kennedy, J. D. *Chem. Commun.* **1999**, 18, 1905.
- (11) Olsen, F. P.; Vasavada, R. C.; Hawthorne, M. F. *J. Am. Chem. Soc.* **1968**, *90*, 3946.
- (12) (a) Gaines, D. F.; Nelson, C. K.; Steehler, G. A. *J. Am. Chem. Soc.* **1984**, *106*, 7266. (b) Wallbridge, M. G. H.; McAvoy, J. S. *J. Chem. Soc., Chem. Commun.* **1969**, 1378. (c) Bould, J.; Greenwood, N. N.; Kennedy, J. D. *Polyhedron* **1983**, *2*, 1401. (d) Brewer, C. T.; Grimes, R. N. *J. Am. Chem. Soc.* **1985**, *107*, 3552. (e) Lawrence, S. H.; Wermer, J. R.; Boocock, S. K.; Banks, M. A.; Keller, P. C.; Shore, S. G. *Inorg. Chem.* **1986**, *25*, 367. (f) Dobson, J.; Keller, P. C.; Schaeffer, R. *Inorg. Chem.* **1968**, *7*, 399. (g) Plešek, J.; Hermanek, S.; Stibr, B.; Hanousek, F. *Collect. Czech. Chem. Commun.* **1967**, *32*, 1095.

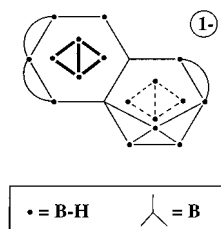


Figure 2. Structure of $B_{19}H_{20}^-$ in stick form. Arcs represent bridging hydrogens.

so as to impart a center of symmetry. The *syn*- $B_{18}H_{22}$ isomer, in which the two cluster fragments are fused in a similar way to yield overall C_2 symmetry, has also been characterized.⁶ The boron atoms common to both cluster fragments in each isomer lack terminal hydrogens. *Syn*- and *anti*- $B_{18}H_{22}$ are diprotic acids forming the anions $B_{18}H_{21}^-$ and $B_{18}H_{20}^{2-}$ by loss of one and two of the six bridge hydrogens, respectively.^{11,13}

Recent developments in the area of rational cluster enlargement¹⁴ utilizing the reactive *nido* decaborane(14) dianion $B_{10}H_{12}^{2-}$ have led us to investigate the octadecaborane(22) system. Although the decaborane-like dianion $B_{18}H_{20}^{2-}$ is less reactive than $B_{10}H_{12}^{2-}$, it has been shown that transition metal moieties can be inserted into the 18-vertex framework to generate 19-vertex metallaboranes in low to moderate yield.⁹ As a result it seemed that 19-vertex boron hydrides could be generated by insertion of monoboron moieties into the dianion $B_{18}H_{20}^{2-}$ to yield the first known nonadecaborate clusters. Herein we report the synthesis and characterization of the anions 10-R- $B_{19}H_{19}^-$ (R = H, Thx), and the dianion $B_{19}H_{19}^{2-}$, by the extension of decaborane cluster growth strategies to the octadecaborane(22) system.

Experimental Section

All experiments were carried out using standard inert atmosphere techniques unless otherwise stated. NaH (60% in mineral oil; Aldrich Chemical Co.) and KH (35% in mineral oil; Aldrich) were washed with dry hexanes prior to use. THF (Na/anthracene), CH_3CN (CaH₂), and pentane (CaH₂) were distilled from the indicated drying agent prior to use. Anhydrous Et₂O (Mallinckrodt) was used as received. $B_{18}H_{22}$ was synthesized by the literature method.^{12a} Proton Sponge (1,8-bis-(dimethylamino)naphthalene), chloroborane–dimethyl sulfide, and dichloroborane–dimethyl sulfide were purchased from Aldrich Chemical Co. and used as received. ThxBHCl·SMe₂ (Thx = tertiary hexyl, $(CH_3)_2CH-C(CH_3)_2$) was synthesized by reaction of 2,3-dimethyl-2-butene with neat $H_2BCl-SMe_2$ at 0 °C for 2 h. ¹¹B NMR spectra were acquired on a Varian Unity 500 (160.4 MHz) or Bruker AM-360 (115.5 MHz) spectrometer and referenced externally to $BF_3 \cdot OEt_2$ in C_6D_6 (δ = 0). Negative mode MALDI-TOF mass spectra were acquired on a Bruker Reflex II spectrometer equipped with a nitrogen laser in reflectron mode using dithranol (1,6-dihydroxynaphthalene; Aldrich Chemical Co.) as a matrix.

One-Pot Synthesis of $B_{19}H_{20}^-$ Using $HBCl_2 \cdot SMe_2$. A 50 mL Schlenk flask containing a stir bar was charged with excess NaH. Solid $B_{18}H_{22}$ (0.29 g, 1.33 mmol) was added under nitrogen in a glovebag. Upon addition of dry Et₂O (25 mL) by syringe, hydrogen evolution was observed and the flask contents turned yellow. $Na_2B_{18}H_{20}$ precipitated as the flask contents were stirred vigorously overnight. $HBCl_2 \cdot SMe_2$ (0.93 g, 6.46 mmol) was added to the slurry by syringe, immediately producing a dark orange-yellow color. The flask was stirred for 6 h, after which the contents were filtered through a medium glass frit and the solids washed with THF until the filtrate was colorless. The filtrate was transferred to a 250 mL Schlenk flask, and the volatile

components were removed under vacuum. Metathesis with $[Ph_3PMe]Br$ in CH_3CN and subsequent reprecipitation from CH_2Cl_2/Et_2O provided 0.47 g (0.93 mmol, 73% yield) of ¹¹B NMR pure $Ph_3PMe[B_{19}H_{20}]$ as a free-flowing yellow powder. MALDI-MS, calcd (obsd): 226.3 (228.3) *m/z*.

Preparation of $B_{19}H_{20}^-$ Using $H_2BCl \cdot SMe_2$. A 50 mL Schlenk flask containing a stir bar was charged with excess KH and $B_{18}H_{22}$ (0.42 g, 1.94 mmol). Dry THF (25 mL) was added, and the contents were stirred on the Schlenk line for 2 h to yield a green-yellow solution. The slurry was filtered into a 100 mL Schlenk flask containing a stir bar, and the volatile components were removed in vacuo to yield a yellow solid. Et₂O (40 mL) was syringed into the flask to generate a slurry prior to addition of $H_2BCl \cdot SMe_2$ (1.01 g, 9.18 mmol) by syringe. The yellow solid dissolved, and the solution slowly turned a lemon-yellow color with formation of a white precipitate. The flask contents were stirred overnight. Hexanes (25 mL) were added, and the flask was allowed to stand until precipitation was complete. The supernatant was removed by filtration, and the precipitate was extracted with CH_3CN until the filtrate was colorless. The potassium cation was displaced in CH_3CN by addition of $[Ph_3PMe]Br$. After filtration and reprecipitation from CH_2Cl_2/Et_2O , the product $Ph_3PMe[B_{19}H_{20}]$ was recovered as a yellow powder in 80% yield (0.52 g, 1.02 mmol) based on starting $B_{18}H_{22}$.

Preparation of 10-Thx- $B_{19}H_{19}^-$. The reaction procedure is identical to that presented in the preceding paragraph with substitution of ThxBHCl·SMe₂ for $H_2BCl \cdot SMe_2$. The compounds were used in the following amounts: $B_{18}H_{22}$ (0.30 g, 1.39 mmol), 2,3-dimethyl-2-butene (5 mL), $H_2BCl \cdot SMe_2$ (0.91 g, 8.24 mmol). Yield: $Et_4N[ThxB_{19}H_{19}]$ (54%, 0.329 g, 0.76 mmol). MALDI-MS (negative mode), calcd (obsd): 310.4 (312.4) *m/z*.

Reaction of $Ph_3PMe[B_{19}H_{20}]$ with Proton Sponge. An excess of Proton Sponge (0.67 g, 3.13 mmol) was added to a THF solution (40 mL) of $Ph_3PMe[B_{19}H_{20}]$ (0.274 g, 1.26 mmol, of $B_{18}H_{22}$; 0.61 g, 5.52 mmol, of $CIBH_2 \cdot SMe_2$; 0.46 g, 1.29 mmol of $[Ph_3PMe]Br$) in a 100 mL three-necked flask. The contents were stirred overnight. The pot mixture contained a yellow solution with a light-colored precipitate. The volatile components were removed under vacuum and the solids washed with 100 mL of Et₂O to remove any residual Proton Sponge. The flask contents were filtered, and the solids were washed with 30 mL portions of dry CH_3CN until the washings were colorless. The filtrate was transferred to a 200 mL Schlenk flask and concentrated under vacuum. The contents were reprecipitated once from CH_3CN/Et_2O , and once from CH_2Cl_2/Et_2O , to give 0.488 g (0.68 mmol, 54% yield based on $B_{18}H_{22}$) of $PSH[Ph_3PMe][B_{19}H_{19}]$.

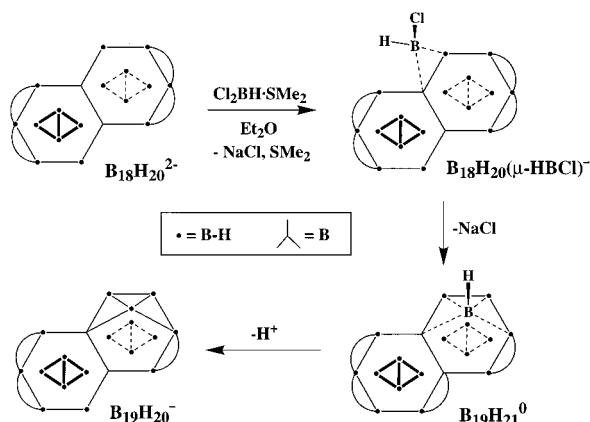
Crystallographic Characterization of $[(Ph_3P)_2N][B_{19}H_{20}] \cdot 0.5THF$. Crystals suitable for analysis were grown by layering a CH_3CN solution of the product with a 1:1 (v/v) mixture of Et₂O/pentane. A yellow crystalline plate (dimensions 0.44 × 0.12 × 0.04 mm) was selected. Intensity data were collected at 133(2) K using a Siemens SMART CCD area detector¹⁵ mounted on a Siemens P4 diffractometer equipped with graphite-monochromated Mo K α radiation (λ = 0.710 73 Å). Unit cell parameters were determined from a nonlinear least-squares fit of 6450 peaks in the range $3.0 < \Theta < 25.0^\circ$. The first 50 frames were repeated at the end of data collection and yielded a total of 286 peaks showing a variation of −0.12% during the data collection. The data were corrected for absorption by the empirical method,¹⁶ giving minimum and maximum transmission factors of 0.738 and 0.956, respectively. The data merged to form a set of 10 670 independent data with $R(int)$ = 0.0483.

The triclinic space group $P\bar{1}$ was determined by statistical tests and verified by subsequent refinement. The structure was solved by direct methods and refined by full-matrix least-squares methods on F^2 .¹⁷ Hydrogen atom positions were initially determined by geometry and refined using a riding model. Non-hydrogen atoms were refined with

- (13) Fontaine, X. L. R.; Greenwood, N. N.; Kennedy, J. D.; MacKinnon, P. *J. Chem. Soc., Dalton Trans.* **1988**, 1785.
(14) Bridges, A. N.; Hayashi, R. K.; Gaines, D. F. *Inorg. Chem.* **1994**, *33*, 1243. Bridges, A. N.; Gaines, D. F. *Inorg. Chem.* **1995**, *34*, 4523.

- (15) (a) Data collection: SMART Software Reference Manual, Siemens Analytical X-ray Instruments, 6300 Enterprise Dr., Madison, WI, 53719-1173, 1994. (b) Data reduction: SAINT Software Reference Manual, Siemens Analytical X-ray Instruments, 6300 Enterprise Dr., Madison, WI 53719-1173, 1995.
(16) G. M. Sheldrick, SADABS, Program for Empirical Absorption Correction of Area Detector Data, University of Göttingen, Germany, 1996.

Scheme 1



anisotropic displacement parameters. A total of 564 parameters were refined against 21 restraints and 10 670 data to give $R_w(F^2) = 0.1934$ and $S = 1.086$. The final $R(F)$ was 0.0645 for the 6940 observed [$F > 4\sigma(F)$] data. The largest shift/su (standard uncertainty) was 0.141 in the final refinement cycle. The final difference map had maxima and minima of 0.889 and $-0.450 \text{ e}/\text{\AA}^3$, respectively.

Results and Discussion

Haloborane–dimethyl sulfide adducts react with $M_2B_{18}H_{20}$ ($M = Na, K$) in diethyl ether to generate the new boron hydride anions $10-R-B_{19}H_{19}^-$ ($R = H, Thx$). This insertion process yields products which are structurally related to the previously reported 19-vertex metallaboranes.⁹ Interestingly, the product may be acquired using either $ClBH_2 \cdot SME_2$ or $Cl_2BH \cdot SME_2$, suggesting that the product is accessible by two independent routes.

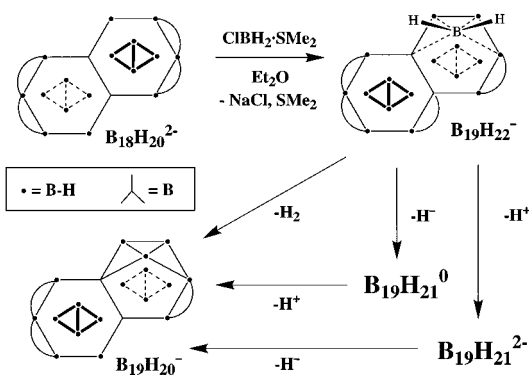
The reaction of excess $Cl_2BH \cdot SME_2$ with $B_{18}H_{20}^{2-}$ in the presence of MH ($M = Na, K$) in diethyl ether generates the product anion $B_{19}H_{20}^-$ (Figure 2), in a convenient one-pot synthesis. Subsequent cation metathesis and recrystallization produced $Ph_3PMe[B_{19}H_{20}]$ in 73% yield. Reactions carried out in the absence of base gave a near 1:1 mixture of the $B_{19}H_{20}^-$ product and $B_{18}H_{21}^-$ as verified by ^{11}B NMR. We propose that the dependence of the yield of $B_{19}H_{20}^-$ on the presence of base is the result of the formation of the unobserved neutral intermediate $B_{19}H_{21}$.

Insertion of a BH_2^{2+} moiety into $B_{18}H_{20}^{2-}$ to make $B_{19}H_{21}$ followed by deprotonation would lead to the formation of $B_{19}H_{20}^-$ (Scheme 1). While $B_{18}H_{20}^{2-}$ may act as a proton acceptor due to its much greater solubility in diethyl ether over MH, the resulting $B_{18}H_{21}^-$ is deprotonated by MH and recycled into the reaction process as $B_{18}H_{20}^{2-}$. It has been postulated that $B_{10}H_{12}^{2-}$ and $B_{10}H_{13}^-$ act as deprotonating agents in cluster enlargement reactions in the presence of MH for the decaborane-(14) system.¹⁴

Reactions of $ClBH_2 \cdot SME_2$ with $B_{18}H_{20}^{2-}$ also generate $B_{19}H_{20}^-$, which may be isolated after cation metathesis with $[Ph_3PMe]Br$ in 80% yield. No base is required to achieve high yields of the product by this method. Attempts to synthesize $B_{19}H_{20}^-$ over NaH in one pot using $ClBH_2 \cdot SME_2$ in analogous fashion to chemistry utilizing $Cl_2BH \cdot SME_2$ were unsuccessful, producing $B_{18}H_{21}^-$ as the primary boron-containing species in solution.

Three pathways may be reasonably proposed for the formation of $B_{19}H_{20}^-$ from monochloroborane and $B_{18}H_{20}^{2-}$ (Scheme 2).

Scheme 2



In the first, loss of halide from $ClBH_2 \cdot SME_2$ allows a BH_2^{2+} unit to add as a bridging moiety and form the unobserved intermediate $B_{19}H_{22}^{2-}$. Loss of molecular hydrogen leads to formation of the $B_{19}H_{20}^-$ product. The isolation of hydrogen generated by the reaction of $K_2B_{18}H_{20}$ with $ClBH_2 \cdot SME_2$ on a high-vacuum line consistently showed ca. 0.13 equiv of H_2 . Thus, hydrogen elimination is not a primary route toward product formation.

A second pathway requires formation of $B_{19}H_{22}^{2-}$ and transfer of H^- to $ClBH_2 \cdot SME_2$ to make $BH_3 \cdot SME_2$, $B_{19}H_{21}$, and MCl . The $B_{19}H_{21}$ is then deprotonated to form the product. This second pathway would be indistinguishable from a third route in which deprotonation of $B_{19}H_{22}^{2-}$ precedes hydride transfer. In reactions of $K_2B_{18}H_{20}$ with $ClBH_2 \cdot SME_2$, $BH_3 \cdot SME_2$, and $B_{18}H_{22}$ are present in the reaction mixture, consistent with the postulate that hydride transfer may be significant. The hydrogen measured may be produced by the reaction of the proposed intermediate $B_{19}H_{22}^{2-}$ with a proton source such as $B_{18}H_{22}$, $B_{18}H_{21}^-$, or $B_{19}H_{21}$. It may be possible that $BH_3 \cdot SME_2$ acts as a hydride acceptor, generating BH_4^- . Although no BH_4^- was observed in the pot mixture, the presence of a moderately strong acid such as $B_{18}H_{22}$ would be expected to convert any BH_4^- formed to BH_3 adducts.

These syntheses appear to require diethyl ether as the solvent. While the salts $M_2B_{18}H_{20}$ ($M = Na, K$) are not highly soluble in diethyl ether, reactions in toluene, in which $M_2B_{18}H_{20}$ salts are virtually insoluble, yield no product and effectively preclude the possibility that the reaction occurs heterogeneously. Reactions in THF, in which the $M_2B_{18}H_{20}$ salts are quite soluble, yield no $B_{19}H_{20}^-$ despite the fact that the reactions will proceed in high yield when up to 10% THF (v/v) is introduced into the diethyl ether pot mixture.

Layering of pentane/ether (1:1) onto a THF solution of $[(Ph_3P)_2N][B_{19}H_{20}]$ produced yellow crystalline prisms of $[(Ph_3P)_2N][B_{19}H_{20}] \cdot 0.5THF$, for which an X-ray diffraction study confirmed the 19-vertex framework (Figure 3). A summary of crystallographic information may be found in Table 1. The anion exists as edge-sharing 10- and 11-vertex *nido* fragments whose open faces are *anti* to one another. Bridge hydrogens span the B9–B10 edge of the 11-vertex subunit, and the B12–B13 and B13–B14 edges of the 10-vertex subunit in a fashion similar to that of $B_{10}H_{14}$. As a result, none of these bridging hydrogens are adjacent to the boron atoms common to both cluster fragments in the solid state. The B–B distances range from 1.626 Å (B4–B8) to 2.032 Å (B11–B12), with an average B–B distance of 1.79 Å. In general, the interatomic distances and angles within the cluster are unexceptional. By inspection, the B10 vertex, located on the open face of the 11-

(17) (a) G. M. Sheldrick, SHELXTL Version 5 Reference Manual, Siemens Analytical X-ray Instruments, 6300 Enterprise Dr., Madison, WI 53719-1173, 1994. (b) *International Tables for Crystallography*; Kluwer: Boston, 1995; Vol. C, Tables 6.1.1.4, 4.2.6.8, and 4.2.4.2.

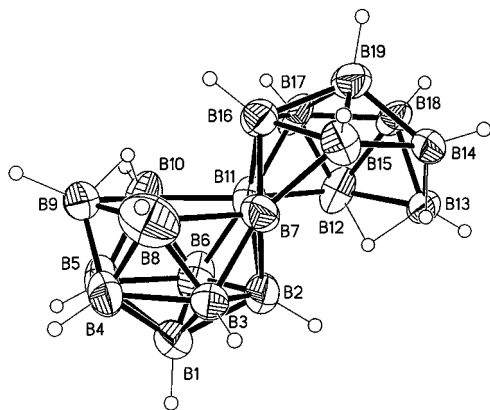


Figure 3. Crystallographically determined structure of $[(\text{Ph}_3\text{P})_2\text{N}][\text{B}_{19}\text{H}_{20}]$ with thermal ellipsoids drawn at the 50% probability level.

Table 1. Summary of Crystallographic Information for $[(\text{Ph}_3\text{P})_2\text{N}][\text{B}_{19}\text{H}_{20}] \cdot 0.5\text{THF}^a$

empirical formula	$\text{C}_{36}\text{B}_{19}\text{N}_4\text{P}_2\text{H}_{50} + 0.5(\text{C}_4\text{H}_8\text{O})$	γ	73.253(2)
fw	800.15	$V, \text{\AA}^3$	2260.25(6)
cryst syst	triclinic	Z	2
space group	$P\bar{1}$ (no. 2)	ρ (calcd), Mg/m^3	1.176
$a, \text{\AA}$	12.6344(2)	μ, mm^{-1}	0.128
$b, \text{\AA}$	13.5978(2)	T, K	133
$c, \text{\AA}$	14.1401(2)	$\lambda, \text{\AA}$	0.71073
α, deg	77.402(2)	R	0.064
β, deg	81.351(2)	R_w	0.193

$$^a R = \sum ||F_o| - |F_c|| / \sum |F_o|, R_w = \{\sum [w(F_o^2 - F_c^2)^2] / \sum [w(F_o^2)^2]\}^{1/2}.$$

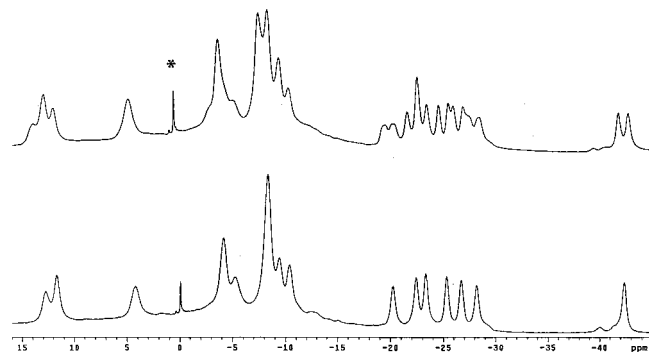


Figure 4. $^{11}\text{B}\{^1\text{H}\}$ (bottom) and ^{11}B (top) NMR (160.4 MHz) spectra of $\text{B}_{19}\text{H}_{20}^-$ in CH_3CN (* = impurity).

vertex subunit, is expected to be the inserted boron atom as notional removal of that vertex regenerates the *anti*- $\text{B}_{18}\text{H}_{22}$ framework.

The ^{11}B NMR spectrum of $\text{B}_{19}\text{H}_{20}^-$ indicates an asymmetric species with chemical shifts ranging from +14 to -42 ppm as illustrated in Figure 4. The common vertexes which lack terminal hydrogens appear as singlets in the proton-coupled spectrum, while all other resonances appear as doublets. The resonances due to the B10 (55 Hz) and B8 (49 Hz) vertexes exhibit bridge hydrogen coupling. Although accidental equivalences prevent the measurement of $J_{\text{B-H}}$ for some cluster atoms, an assignment of the ^{11}B NMR spectrum consistent with the structure was obtained from the ^{11}B - ^{11}B COSY NMR spectrum (Figure 5).

The alkylated 19-vertex derivative $10\text{-Thx-B}_{19}\text{H}_{19}^-$ was isolated as the Et_4N^+ salt in 54% yield from the reaction of $\text{ThxBHCl} \cdot \text{SMe}_2$ with $\text{B}_{18}\text{H}_{20}^{2-}$ in diethyl ether. The ^{11}B NMR spectrum is similar to that for the $\text{B}_{19}\text{H}_{20}^-$ parent (Figure 6). Assignments consistent with the ^{11}B - ^{11}B COSY NMR spectrum indicate that the B10 resonance is shifted downfield by ca. 14

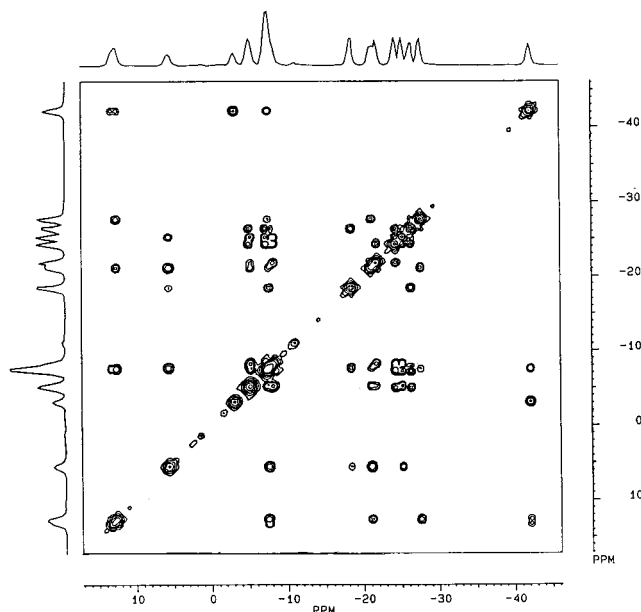


Figure 5. ^{11}B - ^{11}B COSY NMR (160.4 MHz) spectrum of $\text{B}_{19}\text{H}_{20}^-$ in CH_3CN . The 160.4 MHz $^{11}\text{B}\{^1\text{H}\}$ NMR spectrum is plotted on the vertical and horizontal axes.

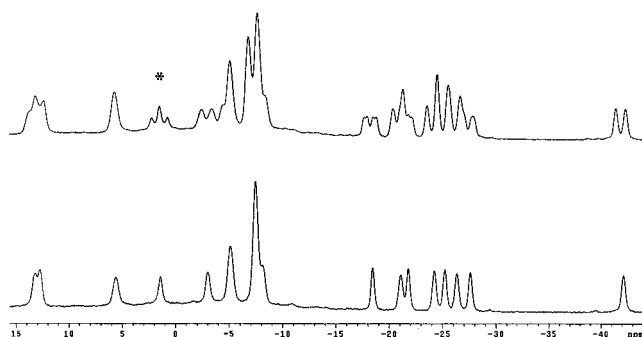


Figure 6. ^{11}B (bottom) and $^{11}\text{B}\{^1\text{H}\}$ (top) NMR (160.4 MHz) spectra of $10\text{-Thx-B}_{19}\text{H}_{19}^-$ in CH_3CN (* = impurity).

ppm, consistent with alkylation at that site and further supporting the assertion that B10 is the inserted vertex. A bridge hydrogen coupling of 41 Hz is also observed for the B8 resonance of $10\text{-Thx-B}_{19}\text{H}_{19}^-$, supporting the assertion that the parent and derivative are structurally analogous.

The MALDI mass spectra of the 19-vertex anions support their structures. $\text{B}_{19}\text{H}_{20}^-$ (obsd 228.3 m/z , calcd 226.3 m/z) and $\text{ThxB}_{19}\text{H}_{19}^-$ (obsd 312.4 m/z , calcd 310.4 m/z) both exhibit mass envelopes of $(M + 2)^-$ in their negative mode mass spectra, indicating addition of 2H (calcd 228.4 m/z $\text{B}_{19}\text{H}_{22}^-$; 312.4 m/z $\text{ThxB}_{19}\text{H}_{21}^-$). The formulation $\text{B}_{19}\text{H}_{22}^-$ is not consistent with the observed structure as the addition of two electrons would force one of the cluster fragments to adopt an *arachno* configuration. The addition of hydrogen has been observed in the MALDI mass spectrum of $\text{B}_{10}\text{H}_{13}^-$ under identical conditions.¹⁸ As a result, we conclude that the addition of hydrogen is a function of the mass spectral experiment and occurs due to the presence of the 10-vertex cluster subunit of the analyte.

The nonadecaborate anions are unstable over extended periods in protic media, decomposing over several weeks to mixtures of $\text{B}_{18}\text{H}_{21}^-$ and $\text{B}(\text{OH})_3$. However, the 19-vertex species neither protonate nor significantly decompose with brief exposure to 1 M HCl/ Et_2O . This observation has led to a convenient meth-

(18) Dopke, N. C.; Dopke, J. A. Manuscript in preparation.

odology for the removal of $B_{18}H_{21}^-$ from samples of the product by protonation of the impurity to yield $B_{18}H_{22}$. Extraction of the octadecaborane with nonpolar solvents and recrystallization from CH_3CN/Et_2O afford pure $B_{19}H_{20}^-$. Solutions of $B_{19}H_{20}^-$ are stable to moderate periods of exposure to air or moisture, while solid samples appear indefinitely stable.

Deprotonation of $B_{19}H_{20}^-$ with Proton Sponge (1,8-bis-(dimethylamino)naphthalene) generates the dianion $B_{19}H_{19}^{2-}$. Substitution of strongly nucleophilic bases (alkyllithiums, $[HBEt_3]^-$) for Proton Sponge results in unresolvable contamination of the product with sizable quantities of $B_{18}H_{20}^{2-}$. Solutions of $B_{19}H_{19}^{2-}$ treated with 1 M HCl/Et_2O regenerate $B_{19}H_{20}^-$ with only trace decomposition to $B_{18}H_{21}^-$ (by ^{11}B NMR analysis), supporting the asserted deprotonation of the nonadecaborate.

The dianion $B_{19}H_{19}^{2-}$ is identified by its ^{11}B NMR spectrum, similar to that of the other 19-vertex boron hydrides. The spectrum consists of 19 resonances over a range of +14 to -36 ppm. Presuming a skeletal structure similar to $B_{19}H_{20}^-$, the ^{11}B NMR spectrum may be assigned on the basis of ^{11}B - ^{11}B COSY NMR spectroscopy. ^{11}B NMR chemical shifts for $B_{19}H_{20}^-$, 10- Thx - $B_{19}H_{19}^-$, and $B_{19}H_{19}^{2-}$ are provided in Table 2. The resonance assigned to the B8 vertex of the undecaborate cluster subunit exhibits a large (64 Hz) bridge hydrogen coupling, indicating that deprotonation occurs on the decaborane subunit. The resonances most greatly effected by deprotonation of the nonadecaborate anion are those assigned to the 10-vertex fragment, when compared to $B_{19}H_{20}^-$.

While reactive toward proton sources, the dianion $B_{19}H_{19}^{2-}$ has yet to show greater affinity toward cluster growth than the 19-vertex monoanion. Attempts to enlarge the 19-vertex $B_{19}H_{20}^-$ or $B_{19}H_{19}^{2-}$ anions to generate 20-vertex clusters have proven to be ineffective. No reaction, except decomposition of the borane anion, has been observed. Further investigations into the reactivity of $B_{19}H_{20}^-$ and $B_{19}H_{19}^{2-}$ are currently underway.

Conclusion

Both $Cl_2BH \cdot SMe_2$ and $ClBH_2 \cdot SMe_2$ effectively convert $M_2B_{18}H_{20}$ to the macropolyhedral boron hydride anion $B_{19}H_{20}^-$ in diethyl ether. The analogous reaction utilizing $RBHCl \cdot SMe_2$ generates the nonadecaborate 10-R- $B_{19}H_{19}^-$. Structurally, these new binary boron hydride anions consist of edge-sharing 10- and 11-vertex *nido* fragments. Treatment of $B_{19}H_{20}^-$ with Proton Sponge generates the dianion $B_{19}H_{19}^{2-}$ which converts back to $B_{19}H_{20}^-$ upon treatment with dilute, anhydrous acid. ^{11}B NMR

Table 2. ^{11}B NMR Chemical Shifts (ppm) for $B_{19}H_{20}^-$, Thx - $B_{19}H_{19}^-$, and $B_{19}H_{19}^{2-}$ in CH_3CN Referenced Externally to $BF_3 \cdot OEt_2$ in C_6D_6 , and Recorded at 160.4 MHz^a

	$B_{19}H_{20}^-$	Thx - $B_{19}H_{19}^-$	$B_{19}H_{19}^{2-}$
B1	-5.0 (135)	-8.3	-5.8 (132)
B2	-25.2 (154)	-25.3 (143)	-21.8 (148)
B3	-7.4	-9.4 (144)	-12.1 (149)
B4	-26.4 (160)	-26.7 (147)	-22.4 (129)
B5	-24.2 (142)	-23.3 (125)	-29.7 (136)
B6	-7.9 (124)	-10.4 (157)	-7.5 (136)
B7	5.6	4.2	13.6
B8	-18.4 (142, 49)	-20.3 (135, 41)	-18.2 (130, 64)
B9	-7.4	-5.3 (153)	-3.2 (136)
B10	-21.8 (135, 55)	-8.1	-19.5
B11	-5.1	-4.2	-9.3
B12	-7.4	-8.4	-20.1
B13	-3.0 (152)	-4.1 (128)	-8.3
B14	-7.4	-8.4	-10.9 (155)
B15	-27.6 (136)	-28.2 (153)	-20.7
B16	-21.1 (148)	-22.4 (148)	-22.7
B17	13.2 (138)	12.8 (138)	11.8 (152)
B18	-42.1 (148)	-42.4 (153)	-35.2 (133)
B19	12.8 (141)	11.7 (148)	-1.2 (132)

^a Coupling constants (Hz), where measurable, appear next to the appropriate shift. Boldface atoms represent vertexes common to both cluster fragments.

evidence implies that deprotonation occurs on the 10-vertex subunit of $B_{19}H_{20}^-$. While the mono- and dianions have thus far been resistant to further cluster growth, they provide the opportunity for further enlargement to new macropolyhedral species.

Acknowledgment. We thank Drs. Nancy C. Dopke (University of Wisconsin) and William C. Boggess (University of Notre Dame) for the acquisition of mass spectral data. We also thank the WARF (J.A.D.) and the National Science Foundation (Grants DMR-9121074, CHE-9629688, and CHE-9310428) for partial funding and major departmental instrumentation grants.

Supporting Information Available: Tables giving atomic coordinates, isotropic and anisotropic displacement parameters, bond lengths and angles, hydrogen coordinates, and torsion angles for $[(Ph_3P)_2N][B_{19}H_{20} \cdot 0.5THF]$, an X-ray crystallographic file (CIF format) of the structure of $[(Ph_3P)_2N][B_{19}H_{20}] \cdot 0.5THF$, and the ^{11}B NMR spectrum of $B_{19}H_{19}^{2-}$. This material is available free of charge via the Internet at <http://pubs.acs.org>.

IC990896C